THE JOURNAL OF PHYSICAL CHEMISTRY Letters

Letter

pubs.acs.org/JPCL

Coherent Control of the Photoionization of Pyrazine

Zhan Hu,[†,‡] Sima Singha,[†] Youbo Zhao,[†,∥] Grant E. Barry,[†] Tamar Seideman,[§] and Robert J. Gordon*[,†]

[†]Department of Chemistry, University of Illinois at Chicago, Chicago, Illinois 60607, United States

[‡]Institute of Atomic and Molecular Physics, Jilin University, Changchun 130021, P. R. China

[§]Department of Chemistry, Northwestern University, 2145 Sheridan Road, Evanston, Illinois 60208, United States

Supporting Information

ABSTRACT: Most attempts to control the absorption of resonant light by quantum mechanical interference have been limited to atoms and small molecules with specialized state configurations and selection rules. Here we illustrate experimentally the possibility of creating laser-induced transparencies in complex molecular systems. Our approach takes advantage of the nonadiabatic excited-state dynamics characteristic of polyatomic molecules. Specifically, we show that it is possible to construct femtosecond pulses using a genetic algorithm to suppress the ionization of isolated pyrazine molecules at a prespecified time. The data suggest that transparency is achieved by localization of a wave packet in a region of the coupled S_1/S_2 potential energy surfaces, where a vertical transition to the ionic state is energetically forbidden. This approach is general and does not require prior knowledge of the molecular Hamiltonian.

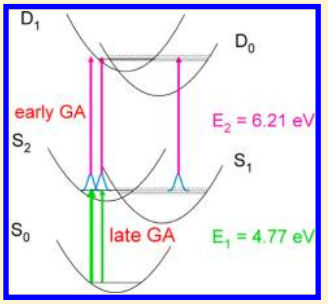

SECTION: Spectroscopy, Photochemistry, and Excited States

In the classical linear regime, the rate of absorption of photons by an atom or molecule is proportional to the number density of the absorbers and the irradiance of the light source. By introducing multiple coherent excitation paths, it is possible to alter the absorption cross section, thereby creating "dark pulses" of light that have the same spectral content as a conventional pulse but are not absorbed by the target species. For example, if a symmetric spectral phase function is imposed on a transform-limited (TL) pulse that is resonant with a two-photon transition, the target may become completely transparent because of destructive interference between red-shifted and blue-shifted components of the pulse.[1] In the case of electromagnetically induced transparency, coherent excitation of a different transition by a controlling pulse can render the sample transparent for the transition of interest.[2] In general, such schemes are restricted to atoms or small molecules with specialized level structures and selection rules and are not easily generalized to complex molecules.

Here we take a different approach to creating dark pulses for large molecules that exhibit complex excited-state dynamics as well as several ionization continua. We focus our attention on the two-color photoionization of an aromatic molecule, in which one pulse excites a neutral electronic state that is coupled to a dark state by a conical intersection, and the second pulse ionizes the molecule after a variable delay, t. We then use a genetic algorithm (GA) to modify the spectral phase of the first pulse, with the objective of suppressing the ion signal at some fixed time, T. By analyzing the growth of the ion signal with the time delay, we seek conditions under which either the first ("pump") or second ("probe") pulse becomes transparent.

As a specific example of an approach that we expect to be general, we chose for this study the photoionization of pyrazine ($C_4H_4N_2$). This molecule has been a case study for numerous experimental[3−9] and theoretical[10−13] investigations of the dynamics of radiationless transitions, and recently there have been a number of theoretical studies of its coherent control.[14−21] The relevant diabatic states are the ground S_0 (^1A_g) state, the first excited singlet S_1($^1B_{3u}$, $n^{-1}\pi^*$) state, and the second excited singlet state S_2 ($^1B_{2u}$, $\pi^{-1}\pi^*$).[22] The energy minima of these states are depicted in Figure 1. The S_1 and S_2

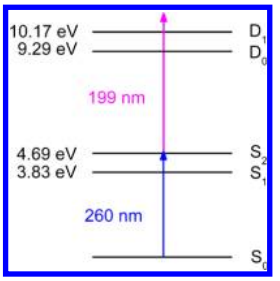

Figure 1. Energy level diagram of pyrazine, showing the photon energies of the pump and probe lasers.

states are vibronically coupled by the 10a (b_{1g}) mode, which promotes internal conversion (IC) in 23 ± 4 fs,[9] as compared with the much slower radiationless decay of S_1 to the ground state, which occurs in 10−20 ps.[5] UV excitation of molecules in the $S_1(n^{-1}\pi^*)$ state produces ions predominantly in the $D_0(n^{-1})$ state, whereas $S_2(\pi^{-1}\pi^*)$ ionizes primarily via the

Received: August 8, 2012
Accepted: September 10, 2012

   dx.doi.org/10.1021/jz301144q | J. Phys. Chem. Lett. 2012, 3, 2744−2748

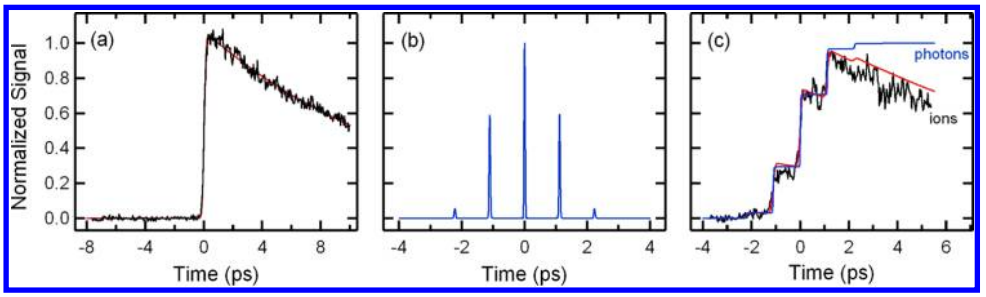

Figure 2. Ion growth curves for some simple pulse shapes. (a) Ion signal versus pump/probe delay time for a transform-limited (TL) pump pulse. The smooth curve is a least-squares fit of the solution to the rate equations. (b) Pulse train produced by a sine phase. (c) Ion growth curve produced by the pulse train shown in panel b. The rate equation curve used the scale factor and decay rate obtained from a TL pulse. The curve labeled "photons" is the fraction of the pulse arriving by time *t*.

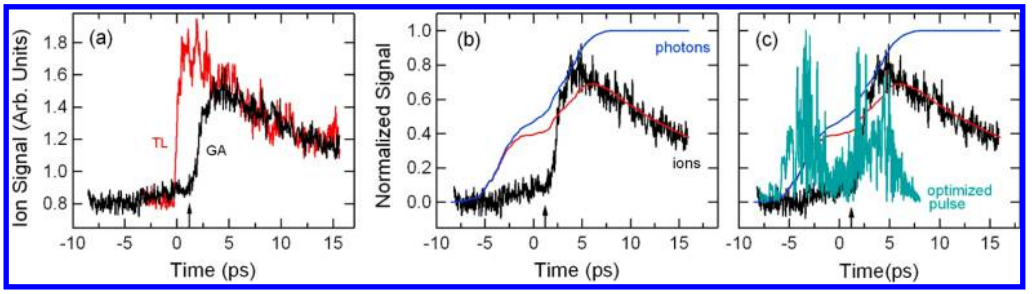

Figure 3. Ion growth curves for the feedback-generated pulse with early target *T*. The arrows at t = 1.24 ps indicate the GA target time. (a) Comparison of the raw data for the GA optimized pulse and a TL pulse measured back-to-back. (b) Comparison of the ion growth curve for the feedback-controlled experiment with the solution to the rate equations. (c) Comparison of the ion growth curve with the optimized pulse envelope.

$D_1(\pi^{-1})$, in accord with a one-electron model for photoionization. Photoelectron measurements indicate that the ratio of the $S_2 \rightarrow D_1$ to $S_2 \rightarrow D_0$ cross sections is approximately 5:1.[9]

The experiment was performed under collision-free conditions. An ultrashort laser pulse centered between 260.5 and 263.6 nm (50 fs, 2.3 nm fwhm, 5×10^{10} W/cm^2) was used to excite an effusive beam of pyrazine to the S_2 state. A 200 nm probe beam (1.1 nm fwhm, $\sim 3 \times 10^{11}$ W/cm^2) ionized the excited molecules after a time delay, *t*, and the parent ions were detected with a time-of-flight mass spectrometer. A key part of the apparatus is an acousto-optic modulator (AOM), which was used to shape the pump pulse by imprinting a spectral phase function, $\Phi(\omega)$, onto the frequency components of the laser beam. The overall time response of the apparatus is 150 fs. Further details of the apparatus are given in the Supporting Information.

Two sets of experiments were performed. In the first, a variety of "simple" pulses were synthesized with the pulse shaper, including a single Gaussian TL pulse, positively and negatively chirped pulses, pulse pairs, and trains of odd numbers of evenly spaced pulses created with a sine phase function. Figure 2a shows the parent ion signal produced by a TL pulse as a function of probe delay. We refer to plots such as this as "ion growth curves." The solid curve is the solution of the classical rate equations describing the reaction sequence

$$S_0 \xrightarrow[I(t)\sigma]{} S_2 \xrightarrow[k_2]{} S_1 \xrightarrow[k_3]{} S_0 \tag{1}$$

namely

$$\frac{dx}{dt} = -I(t)\sigma x + k_3 z \tag{2}$$

$$\frac{dy}{dt} = I(t)\sigma x - k_2 y \tag{3}$$

$$\frac{dz}{dt} = k_2 y - k_3 z \tag{4}$$

where $I(t)$ is the pulse shape (i.e., the envelope of the irradiance), σ is the absorption cross section, and x, y, and z are the number densities of molecules in states S_0, S_2, and S_1, respectively. Because the probe laser is very weak, the ion signal is assumed to vary linearly with the density of the neutral precursors; that is, it is proportional to $\mathrm{Ry}(t) + z(t)$, where R is the relative sensitivity of the probe to S_2 versus S_1. Because $k_2 \gg k_3$, the concentration of S_2 is almost always much smaller than that of S_1, and the ion signal is insensitive to the value of R. In calculating the growth curves, we inserted the known pulse shape of the pump laser into eqs 2 and 3 and averaged over the temporal profile of the probe laser, assuming $1/k_2$ = 23 fs,[9] R = 1.5, and a Gaussian width of 100 fs for the probe. The shape of the pump pulse ($I(t)$) used in the calculation is the calculated output of the AOM. Independent self-correlation measurements of the electric field as well as quantitative agreement between the calculated and measured ion growth curves (e.g., in Figure 2b,c) confirm the fidelity of the pulse shaper. The curve in Figure 2a is a least-squares fit of $\mathrm{Ry}(t) + z(t)$ to the ion signal, treating k_3 and a scale factor as adjustable parameters. In this example, a fitted value of $1/k_3 = 14.3 \pm 0.2$ ps was obtained, which is consistent with the value of 17.5 ± 1 ps in ref 5.

We then went on to test other simple pulse shapes, an example of which is shown in Figure 2b,c. Here a sine phase function[23]

$$\Phi(\omega) = a \sin(b\omega + c) \tag{5}$$

was used, with parameters $a = 0.4\pi$, b = 1132 fs, and c = 0. The resulting pulse shape is plotted in Figure 2b, and the measured ion growth curve is shown in Figure 2c. The spacing of the

dx.doi.org/10.1021/jz301144q | J. Phys. Chem. Lett. 2012, 3, 2744−2748

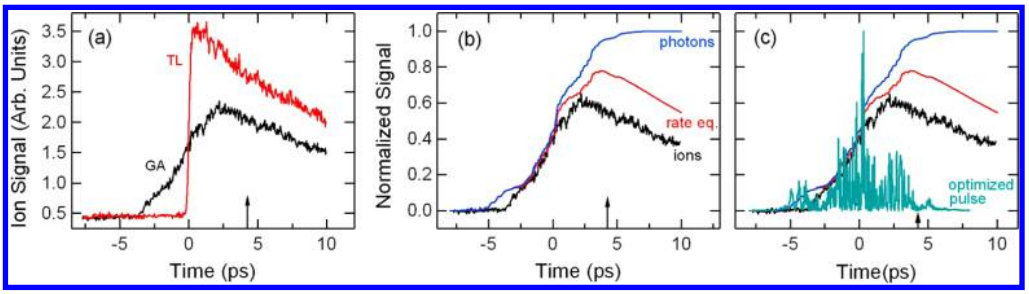

Figure 4. Same as Figure 3, only for T = 4.2 ps.

peaks of the pulse train is much larger than (and not commensurate with[24,25]) the periods of the vibrational modes of the molecule.[22] The calculated ion growth curve in Figure 2c is in excellent agreement with the data. (This comparison confirms that the spacing and relative amplitudes of the subpulses are generated reliably by the AOM.) It is important to emphasize that there are no adjustable parameters in this calculation; the values of k_3 and the scale factor were taken from an independent measurement with a TL pulse. Also shown in Figure 2c is the fraction of the pulse that reaches the molecules at time t (referred to as the "photon growth curve"). We see that the ion growth curve tracks the photon growth curve until decay of the S_1 state sets in. The success of the rate equation model shows that for these simple pulses the data may be accounted for without invoking any coherent effects in the photon absorption and subsequent excited-state dynamics.

In the second set of experiments, a GA[26] was used to program the AOM, with the objective of minimizing the ion signal at a predetermined time, T. Feedback from the ion signal at $t = T$ was used to evolve the laser "genome" until the waveform converged. Two distinct types of behavior were observed, denoted as "early GA" for T as large as 2 ps and "late GA" for much later control points. An example of early GA behavior is shown in Figure 3, where T was set at 1.24 ps. We find that the ion signal is suppressed until $t > T$, after which point the signal rises sharply to the level of the TL growth curve and then decays at the same rate as the TL signal (Figure 3a). The rate equations in this case fail to describe the ion growth at early time, so much so that at $t = 0$ the ion signal is only 10% of its maximum value even though 50% of the photons have arrived (Figure 3b). The optimized pulse shape (Figure 3c) stretches from −8 to +8 ps and has a bimodal envelope with additional substructure. A spectrogram (not shown) of the pulse does not reveal any obvious differences between the two lobes, although very rich phase information presumably encodes different dynamical responses at early and late times. The observation that the ion signals for the TL and GA pulses are identical in the decay region shows that the quantum yields are equal (i.e., the same number of molecules are excited by both pump pulses and are eventually ionized), even though ionization is suppressed prior to the control point.

Strikingly different behavior is observed for the late GA, as illustrated in Figure 4 for T = 4.2 ps. In this case, the ion growth starts ∼1 ps after the onset of the laser pulse and tracks the rate equations fairly well until $t \approx 2$ ps, at which point it falls off and decays at the same rate as the TL case. The quantum yield for the late GA is ∼60% that of the TL pulse, and its pulse shape and spectrogram differ qualitatively from those of the early GA.

Two different types of mechanisms appear to operate for early and late T. For late T, the GA is unable to sustain coherent dynamics, and instead it opts to reduce the effective laser fluence (or, equivalently, it reduces absorption of the pump by molecules in S_0), even though only the spectral phase of the laser pulse is modified. The delayed ionization produced by the early GA could be caused by a number of processes. A trivial explanation is that the GA simply delays the arrival of the laser pulse (e.g., by a linear spectral phase function). This clearly is not the case; just the reverse happens, with the GA pulse starting to arrive 8 ps before the TL pulse. A second possibility is that the first lobe of the genetically optimized pulse reduces absorption by molecules in S_0, and the second one increases it just sufficiently so that the total quantum yield is unchanged. These changes in absorption cross section might be caused by selective excitation of bright states with lower or higher absorption cross sections. To test this hypothesis, we ran a GA with the objective of *increasing* the ion yield at some time T. We found that the GA broadened the pulse and correspondingly stretched out the growth curve but failed to increase the quantum yield. Interestingly, in these runs the rate equations using the optimized pulse shape describe the growth curve quantitatively.

These considerations suggest that the transparency window in the small-T case is due to a coherent mechanism that relies on manipulation of the WP dynamics in the excited manifold. This conjecture is supported by noting that delayed ionization for T < 2 ps is comparable to the calculated ∼0.6 ps vibrational coherence time on the S_1/S_2 surfaces.[10] One possibility is that the GA creates a WP on the S_2 potential energy surface (PES) that is unable to pass through the CI and is trapped in a region where the probe pulse has insufficient energy to induce the $S_2 \rightarrow D_1$ transition. An alternative explanation is that the WP crosses over to the S_1 surface and the $S_1 \rightarrow D_0$ ionization is inhibited. In either case, delayed ionization could occur if the WP is localized on a PES in a region where the probe photon does not have sufficient energy to reach the associated cation PES in a vertical transition. This mechanism was found to account quantitatively for the anomalously rapid decay of the S_1 state of ethylene.[27] There it was shown that the rapid decay of the ion signal was caused by the excited-state WP propagating out of the Franck−Condon window, even though the energy of the probe photon was 4.9 eV above the adiabatic ionization energy. In the present case, where the pump + probe energy exceeds the adiabatic D_1 energy by only 0.83 eV, it is possible that the WP is not ionizable for an initial period. We note that in a photoelectron measurement using a very similar pump/probe configuration with a 22 fs TL excitation pulse, Suzuki et al.[9] observed molecules in the S_2 state prior to IC. The much longer pulses used in the present experiment preclude resolution of such a transient signal, as was also the case in the work of Stert et al.[5]

An interesting question is what might be the mechanism via which the optimal pulse localizes the WP for long periods in a

dx.doi.org/10.1021/jz301144q | J. Phys. Chem. Lett. 2012, 3, 2744−2748

region of a PES that is stable to UV ionization. Coherent control of nonradiative transitions by such a process has been a longstanding goal with many implications. In this quest, Sukharev and Seidman[17] discovered the existence of eigenstates of the total excited states Hamiltonian of molecules undergoing nonradiative transitions, which are localized on the initially excited Born−Oppenheimer surface, a phenomenon analogous to scars of periodic orbits.[28] Using optimal control theory, they predict that it is possible to create laser pulses that localize the system in the bright state indefinitely (>10 ns). The localized eigenstates may be expressed as a superposition of bright states, which the laser pulse is optimized to populate. In the present experiment, it is possible that the GA finds such a superposition. Because of the higher energy of the D_1 state relative to the D_0, it is possible that molecules trapped on the S_2 surface are not as readily ionized by a vertical transition.

Using a similar approach, Christopher et al.[18,19] and Gerbasi et al.[20] expand the bright states as superpositions of eigenstates of the total Hamiltonian. By choosing a suitable linear combination of overlapping bright state resonances, they suppress the $S_2 \rightarrow S_1$ IC over time scales of 50−100 fs. Using this methodology, Grinev et al.[21] are able also to control the $S_0 \rightarrow S_2$ cross section.

In summary, we used an evolutionary algorithm to induce transparency dynamically in the ionization of a complex polyatomic molecule. Strikingly different behaviors were observed in cases where the period over which transparency is desired either exceeds or is smaller than the vibrational dephasing time. In the former case, a transparency window is not achieved, although the total ion yield is reduced. In the latter, the ionization is strongly suppressed over the prespecified period via a coherent mechanism that relies on control of the wave-packet dynamics in the excited manifold via the optimally designed laser pulse. We have shown that even without knowing the molecular Hamiltonian, it is possible to induce transparency by utilizing the complex excited-state dynamics of polyatomic molecules.[29,30] These results are not unique to pyrazine. Given that the excited states of polyatomic molecules are always electronically coupled, a similar mechanism should apply to a large class of molecules.

■ ASSOCIATED CONTENT

Ⓢ Supporting Information

Experimental details are described. This material is available free of charge via the Internet at http://pubs.acs.org.

■ AUTHOR INFORMATION

Corresponding Author

*E-mail: rjgordon@uic.edu.

Present Address

‖Beckman Institute for Advanced Science and Technology, University of Illinois at Urbana−Champaign, 405 North Mathews Avenue, Urbana, IL 61801.

Notes

The authors declare no competing financial interest.

■ ACKNOWLEDGMENTS

We wish to thank Drs. Thomas Weinacht and Marija Kotur for their assistance in setting up the AOM and Drs. Paul Brumer, Wolfgang Domcke, and Moshe Shapiro for fruitful discussions. This work was supported by the National Science Foundation (CHE-0848198) and the National Basic Research Program of China (973 Program) (2013CB922200), National Science Foundation of China (10774056 and 10974070).

■ REFERENCES

(1) Meshulach, D.; Silberberg, Y. Coherent Quantum Control of Two-Photon Transitions by a Femtosecond Laser Pulse. *Nature* **1998**, *396*, 239−342.

(2) Boller, K.-J.; Imamoglu, A.; Harris, S. E. Observation of Electromagnetically Induced Transparency. *Phys. Rev. Lett.* **1991**, *66*, 2593−2596.

(3) Yamazaki, I.; Murao, T.; Yamanaka, T.; Yoshihara, K. Intramolecular Electronic Relaxation and Photoisomerization Processes in the Isolated Azabenzene Molecules Pyridine, Pyrazine and Pyrimidine. *Faraday Discuss. Chem. Soc.* **1983**, *75*, 395−405.

(4) Zhong, D. P.; Diau, E. W. G.; Bernhardt, T. M.; De Feyter, S.; Roberts, J. D.; Zewail, A. H. Femtosecond Dynamics of Valence-Bond Isomers of Azines: Transition States and Conical Intersections. *Chem. Phys. Lett.* **1998**, *298*, 129−140.

(5) Stert, V.; Farmanara, P.; Radloff, W. Electron Configuration Changes in Excited Pyrazine Molecules Analyzed by Femtosecond Time-Resolved Photoelectron Spectroscopy. *J. Chem. Phys.* **2000**, *112*, 4460−4464.

(6) Horio, T.; Fuji, T.; Suzuki, Y. I.; Suzuki, T. Probing Ultrafast Internal Conversion Through Conical Intersection via Time-Energy Map of Photoelectron Angular Anisotropy. *J. Am. Chem. Soc.* **2009**, *131*, 10392−10393.

(7) Tsubouchi, M.; Whitaker, B. J.; Suzuki, T. Femtosecond Photoelectron Imaging on Pyrazine: $S_1 \rightarrow T_1$ Intersystem Crossing and Rotational Coherence Transfer. *J. Phys. Chem. A* **2004**, *108*, 6823−6835.

(8) Liu, S. Y.; Ogi, Y.; Fuji, T.; Nishizawa, K.; Horio, T.; Mizuno, T.; Kohguchi, H.; Nagasono, M.; Togashi, T.; Tono, K.; et al. Time-Resolved Photoelectron Imaging Using a Femtosecond UV Laser and a VUV Free-Electron Laser. *Phys. Rev. A* **2010**, *81*, 031403(R) [1−4].

(9) Suzuki, Y. I.; Fuji, T.; Horio, T.; Suzuki, T. Time-Resolved Photoelectron Imaging of Ultrafast $S_2 \rightarrow S_1$ Internal Conversion Through Conical Intersection In Pyrazine. *J. Chem. Phys.* **2010**, *132*, 174302[1−8].

(10) Schneider, R.; Domcke, W. S_1-S_2 Conical Intersection and Ultrafast $S_2 \rightarrow S_1$ Internal-Conversion in Pyrazine. *Chem. Phys. Lett.* **1988**, *150*, 235−242.

(11) Raab, A.; Worth, G. A.; Meyer, H. D.; Cederbaum, L. S. Molecular Dynamics of Pyrazine After Excitation to the S_2 Electronic State Using a Realistic 24-Mode Model Hamiltonian. *J. Chem. Phys.* **1999**, *110*, 936−946.

(12) Stock, G.; Domcke, W. Femtosecond Spectroscopy of Ultrafast Nonadiabatic Excited-State Dynamics on the Basis of ab-initio Potential-Energy Surfaces: The S_2 State of Pyrazine. *J. Phys. Chem.* **1993**, *97*, 12466−12472.

(13) Stock, G.; Domcke, W. *Femtosecond Time-Resolved Spectroscopy of the Dynamics of Conical Intersections in Conical Intersections Electronic Structure, Dynamics & Spectroscopy*; Domcke, W., Yarkony, D. R.; Köppel, H., Eds.; World Scientific: Singapore, 2004; pp 739−802.

(14) Ferretti, A.; Lami, A.; Villani, G. Control of the Yield of Photophysical Photochemical Processes by Excitation with Properly Delayed Ultrashort Phase-Locked Light-Pulses: A Model Study on the Pyrazine $S_2 \rightarrow S_1$ Internal-Conversion. *Chem. Phys.* **1995**, *196*, 447−454.

(15) Penfold, T. J.; Worth, G. A.; Meier, C. Local Control of Multidimensional Dynamics. *Phys. Chem. Chem. Phys.* **2010**, *12*, 15616−15627.

(16) Wang, L.; Meyer, H.-D.; May, V. Femtosecond Laser Pulse Control of Multidimensional Vibrational Dynamics: Computational Studies on the Pyrazine Molecule. *J. Chem. Phys.* **2006**, *125*, 141202 [1−12].

(17) Sukharev, M.; Seideman, T. Optimal Control Approach to Suppression of Radiationless Transitions. *Phys. Rev. Lett.* **2004**, *93*, 093004 [1−4].

(18) Christopher, P. S.; Shapiro, M.; Brumer, P. Overlapping Resonances in the Coherent Control of Radiationless Transitions: Internal Conversion in Pyrazine. *J. Chem. Phys.* **2005**, *123*, 064313 [1−4].
(19) Christopher, P. S.; Shapiro, M.; Brumer, P. Quantum Control of Internal Conversion in 24-Vibrational-Mode Pyrazine. *J. Chem. Phys.* **2006**, *125*, 124310 [1−9].
(20) Gerbasi, D.; Sanz, A. S.; Christopher, P. S.; Shapiro, M.; Brumer, P. Overlapping Resonances in the Control of Intramolecular Vibrational Redistribution. *J. Chem. Phys.* **2007**, *126*, 124307 [1−9].
(21) Grinev, T.; Shapiro, M.; Brumer, P. Overlapping Resonances Interference-Induced Transparency: The $S_0 \rightarrow S_2/S_1$ Photoexcitation Spectrum of Pyrazine. arXiv:1206.6060v1 (submitted on 26 June 2012).
(22) Innes, K. K.; Ross, I. G.; Moomaw, W. R. Electronic States of Azabenzenes and Azanaphthalenes: A Revised and Extended Critical Review. *J. Mol. Spectrosc.* **1988**, *132*, 492−544.
(23) Hornung, T.; Meier, R; Motzkus, M. Optimal Control of Molecular States in a Learning Loop with a Parameterization in Frequency and Time Domain. *Chem. Phys. Lett.* **2000**, *326*, 445−453.
(24) Voll, J.; de Vivie-Riedle, R. Pulse Trains in Molecular Dynamics and Coherent Spectroscopy: A Theoretical Study. *New J. Phys.* **2009**, *11*, 105306 [1−23].
(25) Singha, S.; Hu, Z.; Gordon, R. J. Closed Loop Coherent Control of Electronic Transitions in Gallium Arsenide. *J. Phys. Chem. A* **2011**, *115*, 6095−6101.
(26) Mitchell, M. *An Introduction to Genetic Algorithms (Complex Adaptive Systems)*; MIT Press: Cambridge, U.K., 2004.
(27) Tao, H.; Allison, T. K.; Wright, T. W.; Stooke, A. M.; Khurmi, C.; van Tilborg, J.; Liu, Y.; Falcone, R. W.; Martinez, T. J.; Belkacem, A. Ultrafast Internal Conversion in Ethylene. I. The Excited State Lifetime. *J. Chem. Phys.* **2011**, *134*, 244306 [1−8].
(28) Heller, E. J. Bound-State Eigenfunctions of Classically Chaotic Hamiltonian Systems: Scars of Periodic Orbits. *Phys. Rev. Lett.* **1984**, *53*, 1515−1518.
(29) Sukharev, M.; Cohen, A.; Gerber, R. B.; Seideman, T. Nonadiabatic Photodissociation Dynamics of F_2 in Solid Ar. *Laser Phys.* **2009**, *19*, 1651−1659.
(30) Sukharev, M.; Seideman, T. Optical Control of Nonradiative Decay in Polyatomic Molecules. *Phys. Rev. A* **2005**, *71*, 012509 [1−10].